Universiteit
Leiden
The Netherlands

Phenotypic screening with 3D cell-based assays

Booij, T.H.

Citation
Booij, T. H. (2017, December 20). *Phenotypic screening with 3D cell-based assays*. Retrieved from https://hdl.handle.net/1887/59503

Version:	Not Applicable (or Unknown)
License:	Licence agreement concerning inclusion of doctoral thesis in the Institutional Repository of the University of Leiden
Downloaded from:	https://hdl.handle.net/1887/59503

Note: To cite this publication please use the final published version (if applicable).

Cover Page

Universiteit Leiden

The following handle holds various files of this Leiden University dissertation:
http://hdl.handle.net/1887/59503

Author: Booij, T.H.
Title: Phenotypic screening with 3D cell-based assays
Issue Date: 2017-12-20

chapter 5

Phenotypic profiling of 3D-cultured micro-tissues to identify selective inhibitors of cyst growth

Tijmen H. Booij[1], Agnieszka Kaczmarczyk[1], Hester Bange[2], Saskia D. van Asten[1], Kuan Yan[2], Bob van de Water[1], Dorien J.M. Peters[3], Leo S. Price[1,2]

1 Division of Toxicology, Leiden Academic Centre for Drug Research (LACDR), Leiden University, Leiden, The Netherlands
2 OcellO B.V., Leiden, The Netherlands
3 Humane Genetica, Leids Universitair Medisch Centrum (LUMC), Leiden, The Netherlands

Manuscript in Preparation

Abstract

Polycystic kidney disease is a relatively frequent monogenetic disorder characterized by the formation of renal cysts that progressively disrupt renal function until the point that patients require dialysis or renal transplantation therapy for survival. Therapeutic options to slow down disease progression are limited, which is partly due to our limited knowledge of the mechanisms contributing to cystogenesis. Additionally, lack of relevant *in vitro* disease models to study cystogenesis has hampered progression in this area.

Here we used a 3D cyst culture screening platform to assess the efficacy of a library of kinase inhibitors with described target specificities. Using phenotypic characterisation, compounds were classified according to phenotypic changes induced by compound intervention, to eliminate potentially cytotoxic compounds. Inhibitor efficacy was related to known molecular targets. Furthermore, to enrich for compounds that specifically inhibited cyst growth, a negative selection was performed in a model for 3D tumour cell invasion.

22 cyst growth inhibitors were retained that could selectively prevent cyst growth without affecting tumour cell morphology. The selected hit compounds targeted, among others, CDK1-9, GSK3, IGF1R/Akt1 and PI3K/Akt1. These results present an opportunity to further investigate therapeutic intervention directed against these targets.

Introduction

Cystogenesis is a process where cells develop into cysts, cell-enclosed cavities, (generally) filled with liquid. While the occurrence of small numbers of individual cysts may not necessarily cause health problems, development and growth of large numbers of cysts can have severe consequences and can be the result of underlying genetic mutations that predispose for cystic disorders. A relatively common cystic disorder is polycystic kidney disease (PKD). This disorder affects approximately 1:2500 people[1] that eventually develop renal failure and require dialysis or a kidney transplant for survival.[2] This slow-developing disease, caused by mutations in the *PKD1* or *PKD2* gene,[3] is notoriously difficult to treat medicinally, due to the plethora of dysregulated cellular signalling pathways.[3-5] The only currently approved therapy in the EU, tolvaptan, slows down cystogenesis but is also known to have side effects both related[6-8] and unrelated[9-11] to its mechanism of action.

A traditional problem associated with this type of disease, where tissue architecture plays a critical role in the pathology, is that conventional two-dimensional (2D) *in vitro* cell monolayers do not provide an adequate context to study drug efficacy. Hence, drugs have generally been tested in animal models that were genetically altered to simulate the pathophysiology.[12-14] However, while such models have improved relevance to the human disease, they cannot be used to assess the efficacy of large quantities of compounds. To bridge this gap between traditional *in vitro* and *in vivo* disease models, more advanced *in vitro* cell culture techniques, in which cells are cultured as three-dimensional (3D) micro-tissues, have been developed in recent years.[15-19] Unfortunately, despite clear benefits of these 3D cell culture models,[17, 20] these are still not used routinely for large-scale drug testing.[21] Another area where these more advanced *in vitro* cell culture models may be essential is the prediction of toxicity of new drugs.[22] Unexpected toxicity is a major problem in drug development resulting in a high level of pre-clinical and clinical failure.[22-25] Especially for chronic disorders such as PKD, where patients require life-long treatment, it is critical that new drugs have a very favourable safety profile. Screening drugs in more advanced and physiologically relevant biological models will reduce pre-clinical failures and may help introduce safer drugs to the market.[26]

To find potential new safe therapeutics for PKD and to unravel mechanisms of cyst growth, we screened a library of 428 kinase inhibitors with well-defined target specificity in an *in vitro* assay for cyst development. We subsequently selected drugs that showed a desirable efficacy and safety profile in this *in vitro* model, and counter-screened these compounds using a 3D tumour cell invasion assay in order to select compounds that specifically inhibited cyst growth. Additionally, we investigated the target specificities of the selected compounds, identifying cyclin-dependent kinases (CDKs), glycogen synthase kinase 3 (GSK3)-α/β, insulin-like growth factor 1 receptor (IGF1R), human epidermal growth factor receptor 2 (HER2), and Akt1 as potential targets for therapeutic intervention.

MATERIALS AND METHODS

Cell Lines

For 3D cyst assays and 2D ATPlite viability measurements (discussed below), mouse inner medullary collecting duct (mIMCD3 ATCC® CRL-2123™) cells harbouring a deletion of the *Pkd1* gene were generated using the dimeric CRISPR RNA-guided FokI nucleases (RFN) method[27] as previously described.[28] These cells are referred to as mIMRFNPKD 5E4 throughout this article. This cell line was maintained in 175cm² culture flasks at 37°C +5% CO2 in DMEM/F12 Ham's culture medium (D8062, Sigma-Aldrich, Zwijndrecht, Netherlands), supplemented with 10% fetal bovine serum (FBS, Gibco™, ThermoFisher Scientific, Landsmeer, Netherlands), glutamax and penicillin/streptomycin. Before cells reached maximum density, the monolayer was washed with 1x PBS (Sigma-Aldrich, Zwijndrecht, Netherlands) and subsequently trypsinized with 1x Trypsin (Gibco™, ThermoFisher Scientific, Landsmeer, Netherlands). Cells were collected in culture medium and pelleted by centrifugation. Cell pellets were resuspended in FBS containing 10% dimethyl sulfoxide (DMSO, Biosolve B.V., Valkenswaard, Netherlands) for cryopreservation at -150°C.

For tumour cell invasion assays, we used the 4T1 murine breast cancer cell line (ATCC® CRL-2539™). 4T1 cells were maintained in RPMI-1640 culture medium supplemented with 10% FBS and 25µg/mL penicillin and streptomycin (Invitrogen™, ThermoFisher Scientific) according to standard procedure. Cells were cryopreserved at -150°C similarly to mIMRFNPKD 5E4 cells in cryopreservation medium (above).

3D cyst culture assay

The 3D cyst assay was performed as previously described.[28] Briefly, frozen mIMRFNPKD 5E4 cells were quick-thawed and cultured in 175cm² flasks 72 hours prior to starting the cyst assay. Growth medium was exchanged after 24 hours and after 72 hours the monolayer was trypsinized according to the procedure described above and the cells were mixed in cold Cyst-Gel (OcellO B.V., Leiden, Netherlands) and plated in 384 well plates, 14.5µL/well, (Greiner µClear, Greiner Bio-One B.V., Alphen aan den Rijn, Netherlands) using a CyBi Selma 96/60 robotic liquid handler (Analyik Jena AG, Jena, Germany). After gel polymerization at 37°C for 30 minutes, 33.5L culture medium was added to each well and small cysts were allowed to develop for a period of 96 hours at 37°C (5% CO_2), after which cells were co-exposed with forskolin (*Coleus Forskohlii*, Calbiochem, Millipore BV, Amsterdam, Netherlands, an activator of adenylyl cyclases to enhance intracellular 3',5'-cyclic adenosine monophosphate (cAMP) levels, which is a known mediator of cyst growth), and test compounds using a CyBi Selma 96/60 liquid handler. After 72 hours of compound exposures, plates were fixed and stained using a solution of 3% formaldehyde (Sigma-Aldrich, Zwijndrecht, Netherlands), 0.2% Triton X-100 (Sigma-Aldrich, Zwijndrecht, Netherlands), 0.25µM rhodamine-phalloidin (Sigma-Aldrich, Zwijndrecht, Netherlands) and 0.1% Hoechst 33258 (Sigma-Aldrich, Zwijndrecht, Netherlands) in 1x PBS for at least 12 hours at 4°C. Subsequently, plates were washed in 1x PBS for 12-24 hours, before sealing with a Greiner SilverSeal (Greiner

Bio-One B.V., Alphen aan den Rijn, Netherlands). The plates were stored at 4°C prior to imaging.

3D 4T1 cell invasion assay

Frozen 4T1 cells were quick-thawed to 37°C and subsequently mixed with a hydrogel mix consisting of Matrigel (BD Biosciences, Breda, Netherlands) and collagen-I (BD Biosciences, Breda, Netherlands) and 14.5µL was transferred to each well of a 384 well plate (Greiner µClear, Greiner Bio-One B.V., Alphen aan den Rijn, Netherlands), using the CyBi Selma 96/60 robotic liquid handler (Analyik Jena AG, Jena, Germany), as previously described.[29] After gel polymerization at 37°C for 30 minutes, 39.5µL RPMI-1640 culture medium (as described above for 4T1 cell maintenance) was added to all wells. Compound exposures were performed immediately using the CyBi Selma 96/60 robotic liquid handler (Analyik Jena AG, Jena, Germany). Cells were subsequently cultured at 37°C (5% CO_2) or 48 hours, prior to fixing and staining as described above for the 3D cyst culture assay.

ATPlite assay

Measurement of cell viability was performed using PerkinElmer's 1-step ATPlite kit (PerkinElmer Nederland B.V., Groningen, Netherlands) according to manufacturer's instructions in 384 well plates. Briefly, mIMRFNPKD 5E4 cells were seeded in 384 well plates 48 hours prior to compound treatments at a final cell density of 1000c/well. After compound exposure, the total volume in each well was kept at 25µL. After 48 hours, 25µL ATPlite reagent was added to all wells and the plates were shaken at 700rpm using an orbital plate shaker. Luminescence readout was performed using a FLUOstar OPTIMA microplate reader (BMG Labtech, Isogen Life Science, De Meern, Netherlands). Luminescence readout was scaled between controls without cells (0%) and solvent condition (100%) using NPI-normalization in KNIME Analytics Platform (KNIME 3.1.2, Konstanz, Germany, http://www.knime.org/ for Microsoft Windows 7).

Compounds

The kinase inhibitor library (Chemical Validation Library, CVL), with compounds predissolved in DMSO, was developed by Vichem Chemie Research Ltd. (Budapest, Hungary).[30-31] Rapamycin, roscovitine, entinostat, dasatinib and sorafenib tosylate were obtained from SelleckChem (Munich, Germany). IBMX (3-isobutyl-1-methylxanthine) was obtained from Cayman Chemical (Sanbio B.V. Uden, Netherlands). 8-Br-cAMP was obtained from Santa Cruz Biotechnology Inc. (Heidelberg, Germany) and Prostaglandin E1 was obtained from Sigma-Aldrich (Zwijndrecht, Netherlands).

Fluorescence Microscopy

3D micro-tissues were stained with Hoechst 33258 and rhodamine-phalloidin as described above and subsequently imaged using a BD Pathway 855 (BD Biosciences, Breda, Netherlands) automated inverted wide-field microscope using a 4x Olympus objective and accompanying BD Attovision software (BD Biosciences, Breda, Netherlands), or an ImageXpress Micro XLS wide field high-content analysis system

(Molecular Devices, Sunnyvale, CA, USA), equipped with a 4x objective. Images were captured in the z-plane at intervals of 50µm. The gel was imaged through its entire depth (z-axis), requiring around 25 images per well per fluorescence channel.

Image analysis and Image Processing

For mIMRFNPKD 5E4 cyst cultures, image stacks were analysed and phenotypes were quantified using Ominer software (OcellO B.V., Leiden, Netherlands) integrated in KNIME Analytics Platform (KNIME 3.1.2, Konstanz, Germany, http://www.knime.org/ for Microsoft Windows 7). This software was used to extract 450 phenotypic measurements of cystic structures as described previously.[28] The phenotypic measurements were subsequently Z-score normalized (to unstimulated control) or NPI-normalized using KNIME software (between unstimulated control, 100%, and forskolin-stimulated controls, 0%) for presentation purposes. Principal component analysis (PCA) was trained on stimulated and unstimulated control groups, and phenotypic features with Z'›0.5 between these groups were retained for PCA training. The trained PCA was subsequently applied over the test data, retaining 3 principal components that preserved 98% of the information. Afterwards, these principal components were used to train clusters based on the K Nearest Neighbour algorithm (k-NN) (3 neighbours to consider) on unstimulated, forskolin-stimulated and staurosporin-treated control groups. The trained classifier was subsequently applied over the test data to classify phenotypic similarities between test compounds and control conditions.

For 4T1 cell tumouroids, Ominer software was used to generate maximum-intensity projections of both Hoechst-33258 and Rhodamine-Phalloidin-derived signals. Phenotypic changes were subsequently quantified using Ominer software as described previously[32]. The phenotypic measurements were subsequently stored as spreadsheets. Using KNIME Analytics Platform version 3.3.1 for Mac OS X El Capitan, all phenotypic measurements were subsequently Z-score normalized to solvent control (0.1% DMSO). PCA was trained on control conditions (untreated, solvent control, dasatinib, entinostat, excluding several texture- and image moment-related phenotypic parameters: Gabor Wavelets, Zernike Moments and Hu Moments). From the resulting PCA model, 3 principal components (retaining 74% variation) were retained and used for phenotypic classification using k-NN classification integrated in KNIME. The classification algorithm was trained on control conditions (untreated, solvent control, dasatinib, entinostat, sorafenib) using standard settings (3 neighbours to consider) and subsequently applied to classify the test compounds.

Percent-inhibition of cyst growth or viability and classification results are presented using heatmap plots where class or magnitude of inhibition is presented as a colour scale. These plots were generated for presentation purposes of large datasets, using the ggplot2 (http://ggplot2.org) package for Rstudio v1.0.136 for Mac OS X El Capitan (https://www.rstudio.com/products/rstudio) with R version 3.3.2 for Mac OS X El Capitan (https://www.r-project.org/). PCA plots were also made using the ggplot2 package. All other plots were generated using Graphpad Prism 7 (Graphpad Software, La Jolla, California, USA).

RESULTS

Cyst growth can be stimulated by cAMP-enhancing agents and blocked by known cyst growth inhibitors

To identify selective inhibitors of cystogenesis, we followed the workflow presented in supplemental figure 1. First, we further characterized a previously developed model for PKD, to determine whether cyst swelling could be induced by known enhancers and whether this could be inhibited by known inhibitors of cyst growth. We investigated whether cyst growth could be increased by exposure of cysts to forskolin at different concentrations in the absence or presence of an inhibitor of cAMP breakdown, IBMX (3-isobutyl-1-methylxanthine) (figure 1A, left panel). Cyst growth was enhanced relative to solvent control (represented by a dotted line), and was not altered due to the influence of IBMX. Similarly, a membrane-permeable cAMP analogue, 8-Br-cAMP, could enhance cyst swelling on its own, but was much more potent when used in combination with 100μM IBMX (figure 1A, middle panel). Prostaglandin E1 can indirectly activate adenylyl cyclases through the prostaglandin receptor, and this also enhanced cyst growth alone and more strongly in combination with IBMX (figure 1A, right panel). For all endpoint conditions, representative images are presented in figure 1B. Cyst swelling induced by forskolin could, in contrast, be inhibited by the actions of compounds that are known to affect pathways involved in cyst growth, such as rapamycin (inhibitor of mammalian target of rapamycin, mTOR[33-38]), roscovitine (inhibitor of cyclin-dependent kinases; CDK1, CDK2, CDK5, CDK7 and CDK9[39-42]) or sorafenib (sorafenib tosylate, vascular endothelial growth factor receptor (VEGFR)/Raf[43-45]) (figure 1C and D).

High-throughput screening of kinase inhibitors identifies inhibitors of forskolin-induced cyst growth

To identify new cyst growth inhibitors and associated molecular targets, we tested a kinase inhibitor library containing 428 kinase inhibitors with varying target specificity for effects on cyst growth. A heat map presenting the known target specificity is included as supplemental figure 2. All compounds were screened at a concentration of 1μM, in triplicate wells, in the presence of 2.5μM forskolin and subsequently ranked according to their inhibitory potential of cyst growth, as measured by cyst area (figure 2A, 100% inhibition corresponds with unstimulated control and 0% inhibition corresponds with 2.5μM forskolin without test compound). Hit compounds were selected that showed ≥50% inhibition of cyst growth for the median of triplicate wells, as visualized in figure 2A by the green shade. The selected 99 compounds were re-screened at 1μM, 100nM and 10nM in triplicate and cyst growth was scaled between 100% inhibition (unstimulated controls) and 0% inhibition (2.5μM forskolin only). DMSO (solvent) was kept at a constant 0.2% throughout all dilutions. The median inhibitory potency of triplicate wells of all compounds is shown in figure 2C as a heatmap, where the colour scale from yellow (no inhibition) to red (strong inhibition of cyst growth) represents the inhibitory potential. Subsequently, 9 of the 99 hits in this secondary screen were rejected as false positives as they failed to inhibit cyst growth by ≥50% at 1μM (the cut-off in the primary screen, figure 2C, excluded compounds from B shown in red).

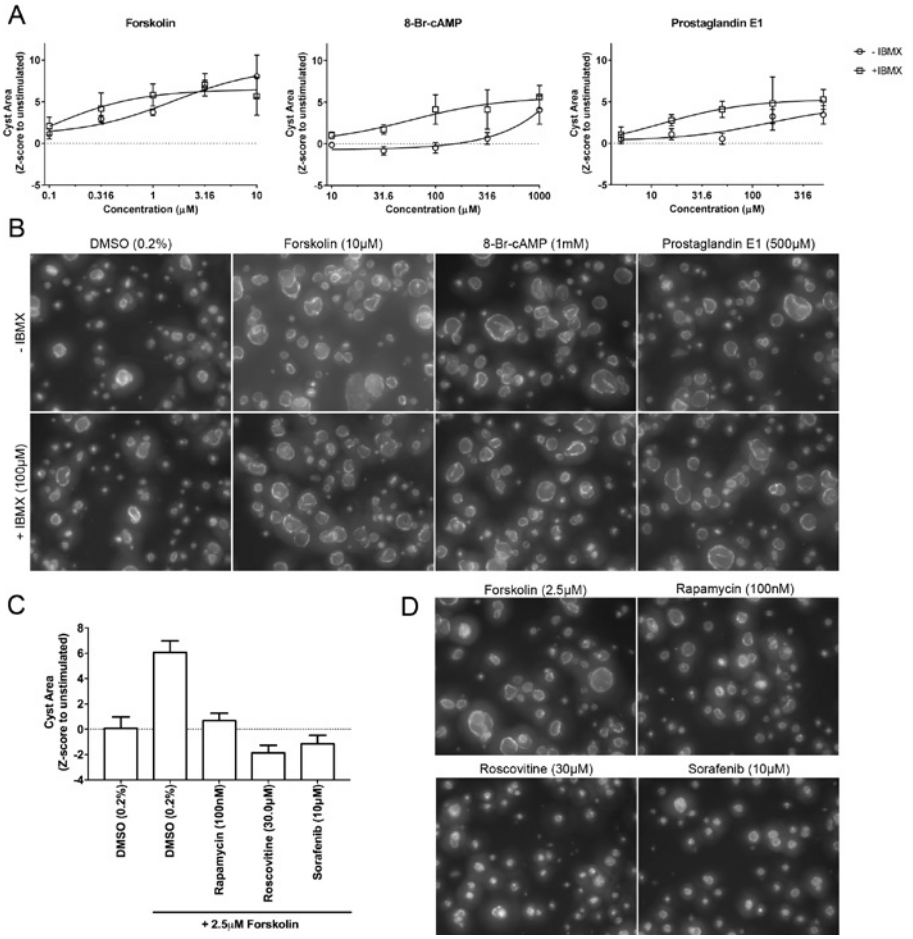

FIGURE 1 Cystogenesis in a 3D-culture assay can be enhanced by cAMP-stimulating agents and inhibited by known inhibitors of cyst growth. **A)** Cystogenesis as measured by cyst size (area) is enhanced as a result of stimulation with forskolin, 8-Br-cAMP or prostaglandin E1 compared to DMSO control, either in the absence of or in the presence of 100μM IBMX (3-isobutyl-1-methylxanthine). Data points represent mean ± SD of quadruplicate wells. **B)** Representative images taken with the BD Pathway 855 imager, Filamentous actin (rhodamine-phalloidin) shown. Top panel represents condition without IBMX and bottom panel represents condition with 100μM IBMX. **C)** Known inhibitors of cyst growth prevent forskolin-induced cyst growth in mIMRFNPKD 5E4 cells. Bars represent means ± SD of ≥4 replicate wells. **D)** Representative images taken with the BD Pathway 855 imager from C). Images in B and D are 700x550px cut-out with enhanced contrast and brightness shown for presentation purposes.

Multiparametric phenotypic analysis of cysts can discriminate between effective, ineffective and potentially toxic effects

It is not possible to exclude potentially toxic compounds by solely using a measurement of cyst size. Since phenotypic analysis can visualise diverse phenotypic changes as a result of compound treatment, including those that may be associated with toxicity, a principal components analysis was trained using known control compounds and applied over the validation screen data. Showing the first two principal components, the different control groups can be discriminated clearly (figure 3A). Interestingly, but quite unsurprisingly, 250nM staurosporin (which was included as a positive control for toxicity) induced a phenotypic change different from all other tested control compounds. We subsequently used this information with the K-nearest neighbour algorithm to classify compound effects according to phenotypic similarity with positive- and negative control conditions. We defined three classes: (i) forskolin-stimulated-like compounds, where the phenotype is similar to the condition without compound added; (ii) similar to positive control compounds, where the phenotype is similar to unstimulated controls or rapamycin/roscovitine/sorafenib-treated cysts and where we expect effective and non-toxic compounds; and, (iii) staurosporin-like phenotypes, where we expected most potentially cytotoxic compounds (figure 3B). As all compounds were tested in triplicate, a compound was assigned to a certain class when at least 2/3 replicates were present in that class; this information was subsequently used to generate figure 3C, where the colours represent phenotypic classification. Of interest, compound VCC41 was revealed to be staurosporin, which was included as an internal control compound in the compound library. This internal control was not used to train the classification algorithm, but still classified as 'staurosporin-like' at all tested concentrations, illustrating the robustness of this classification.

In order to reveal potential effects on cell viability, the compounds were tested in parallel in 2D-cultured mIMRFNPKD 5E4 cells, and viability was assessed using standard ATPlite assay. This showed that compounds classified as inducing a staurosporin-like phenotypic change also often inhibit viability of 2D cultured cells (figure 3D and supplemental figure 3).

Compounds inducing similar phenotypic changes as staurosporin were considered toxic and excluded from further analysis. Since all compounds may induce toxicity at high doses, compounds that inhibited cyst growth at least two lower concentrations without classifying as 'staurosporin-like' were not excluded from further analysis. A few compounds that had previously shown only mild activity at inhibiting cyst growth (<60% inhibition, figure 2B) and also classified as 'similar to forskolin-treated' at all tested concentrations in figure 3C (e.g. VCC16, -84), were excluded due to a lack of potency, resulting in 49 compounds remaining (figure 4A-C). While these compounds did not affect phenotypic changes characteristic of cytotoxicity in 3D, cell viability of 2D-cultured mIMRFNPKD 5E4 cells was influenced as measured by ATPlite assay (figure 4B). Because many of the molecules in this kinase library targeted multiple kinases (figure 4C), it is challenging to link 2D cell viability to molecular targets – although some

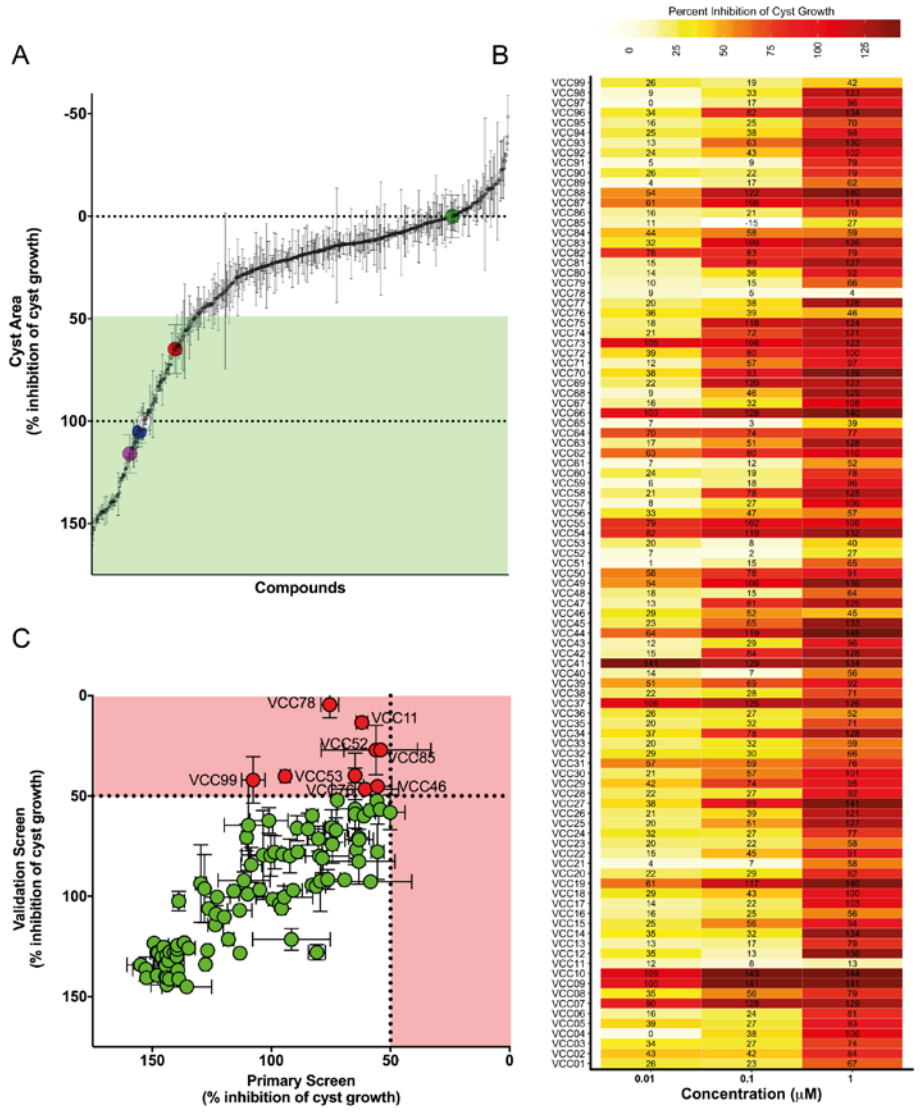

FIGURE 2 Screening a kinase inhibitor library identified inhibitors of cystogenesis. **A)** 428 compounds screened at 1μM concentration in triplicate in the presence of 2.5μM forskolin, alongside control compounds. Unstimulated control condition (0.2% DMSO, n=398) represents 100% cyst growth inhibition and is visualised by a white circle at 100% inhibition. Stimulated controls (2.5μM forskolin, n=500) represent 0% inhibition of cyst growth and are visualised by a green circle at 0% inhibition. Positive control compounds that are known to inhibit cyst growth are presented by enlarged circles in purple (roscovitine, n=24), blue (sorafenib, n=24) and red (rapamycin, n=24). All other data points represent median percent inhibition of triplicate wells ± MAD. Green shaded area contains selected hits (triplicate median ≥50% inhibition).
(legend continues on next page)

B) 99 selected cyst growth inhibitors rescreened at 1µM, 100nM and 10nM in triplicate. Median cyst growth inhibitory activity of triplicate wells is presented as a heatmap with colour scale from light yellow (no inhibition) to bright red (strong inhibition). Percent inhibition of cyst growth is included as numeric value in the heatmap plot. **C)** Comparison of compound activity between primary screen and validation screen at 1µM concentration. 9 compounds failed to show sufficient activity (≥50% inhibition) and were therefore excluded from further analysis. Data points represent median values of primary- and validation screen. Horizontal error bars represent MAD from primary screen and vertical error bars represent MAD from validation screen. Included compounds shown as green circles; compounds excluded shown as red circles.

molecules (e.g. VCC50) that cause a reduction of cell viability also target a wider range of different kinases. Since the 3D cyst assay did not indicate potential cytotoxic effects of these molecules, we reasoned that these effects may be specific to 2D-cultured cells and therefore decided to use a different 3D assay for the prioritization of compounds.

Counter-screening with 3D-cultured 4T1 breast cancer cells to select selective inhibitors of cystogenesis

To discriminate compounds that have an effect on cyst swelling from more general processes that may affect cyst size, such as proliferation and cell adhesion, we also screened the same kinase inhibitor library on a 3D cancer cell invasion model.[29] Compounds that inhibited cyst swelling but did not induce changes in the morphology of 4T1 breast cancer cells cultured in 3D (which do not form cystic structures), were classified as inhibitors of cyst growth independent of more general cellular processes.

Figure 5A shows representative images of 3D-cultured 4T1 cells under control conditions. Consistent with previous results,[14] unstimulated and solvent control conditions revealed small clumps of 4T1 cells expressing ('invasive') branching morphology. In contrast, dasatinib-treated 4T1 cells failed to invade into the surrounding matrix and formed round multicellular spheroids. Sorafenib and entinostat similarly prevented branching morphogenesis, but probably inhibited the growth rate of these spheroidal clumps as judged by reduced structure size.

Analogous to the multiparametric classification approach followed for mIMRFNP-KD 5E4-based analysis, we trained a PCA on 4T1 control phenotypes (first two principal components shown in figure 5B, showing all data points), and subsequently used the K-nearest neighbour algorithm to classify all data points according to the control classes. The trained cluster algorithm was subsequently applied over the Vichem compounds as shown in figure 5C (circles represent median of quadruplicate wells). This showed that a large proportion of the screened compounds affected 4T1 phenotypes. From these compounds, we further analysed those that were previously identified as inhibitors of cystogenesis as shown in figure 4A. The classification of these compounds according to efficacy on 4T1 cells is presented in figure 5D, and the corresponding PCA

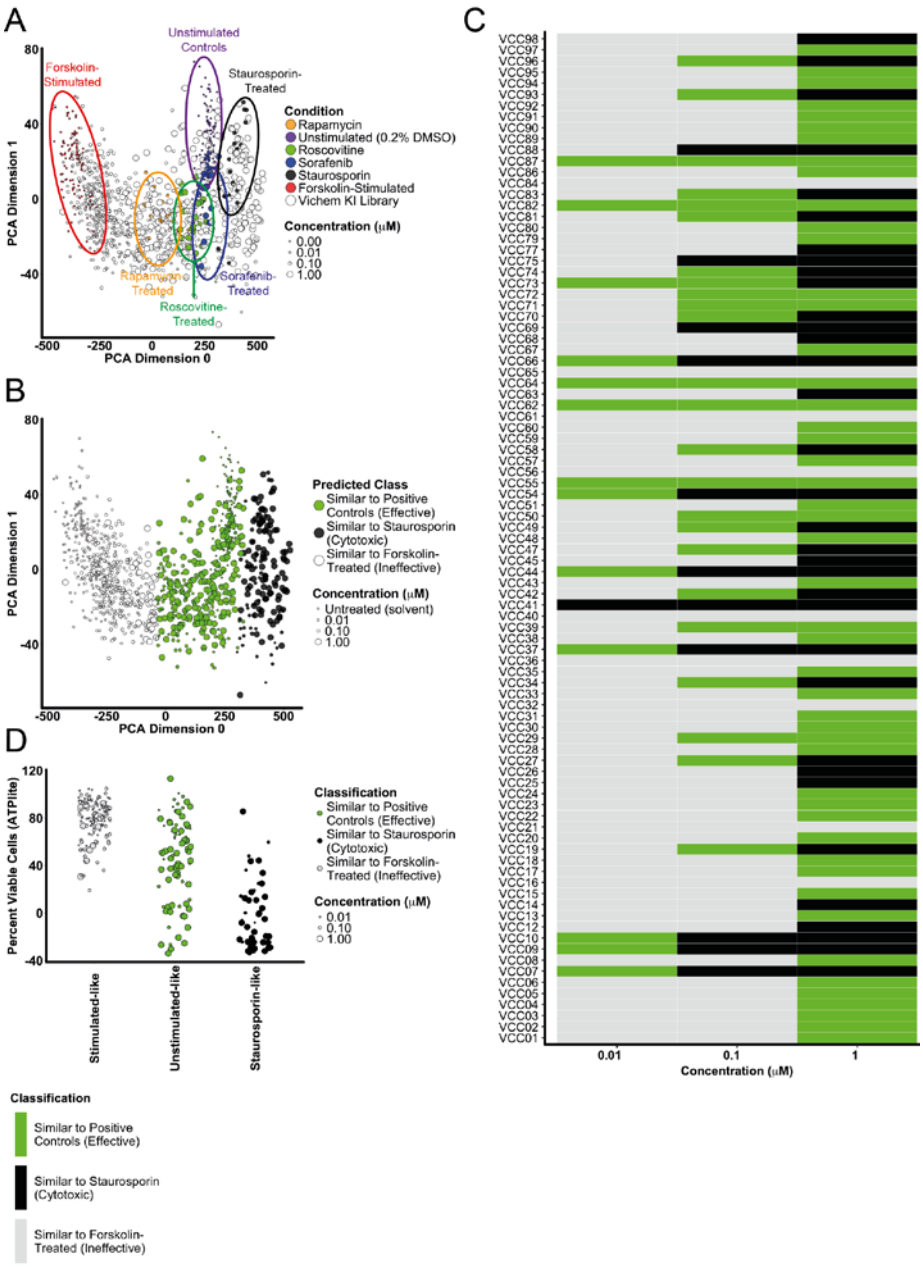

FIGURE 3 **Phenotypic classification can be used to identify effective and non-toxic compounds. A)** PCA was trained on control groups (marked by circles in plot) and subsequently applied to the full dataset. Phenotypic space separates unstimulated (purple) and other positive control compounds (rapamycin, roscovitine, sorafenib) from stimulated (red) controls. Circles represent individual wells. First two principal components shown **B)** K nearest neighbour classification using the first three principal

(legend continues on next page)

components discriminates effective (green), ineffective (white), and cytotoxic (black) compounds. Circles represent individual wells. First two principal components shown for presentation purposes. **C)** Heat map showing classification of compounds when ≥2/3 replicates belong to that class. Black colour represents cytotoxic compounds, green represents efficacy and light grey colour represents inactive. **D)** ATPlite measurement of 2D-cultured mIMRFNPKD 5E4 cells after compound classification. Staurosporin-like data points more often inhibit viability.

plot is shown as figure 5E. Several of the inhibitors of cystogenesis that were identified using mIMRFNPKD 5E4 cells also apparently affected 4T1 cell morphology. Therefore, in order to select solely compounds that affected cystogenesis but not 4T1 phenotype, we selected for compounds that could inhibit cystogenesis at concentrations where 4T1 phenotype was unaffected. This stringent selection resulted in 22 compounds that potently inhibited cyst growth, but did not affect the phenotype of 4T1 cells in 3D. Although many of these compounds did not have targets described with IC50's below micromolar range, six inhibitors targeted various CDKs, whereas others dual-targeted Akt1/ IGF1R, phosphatidylinositol-4,5-bisphosphate 3-kinase (PI3K)/Akt1 or GSK3-alpha/beta and CDKs (Table 1).

Prioritization of selected compounds using 2D cell viability measurements

Since the compounds that were selected to solely inhibit cyst growth, but not change 4T1 phenotypes may still inhibit 2D cell viability, we plotted dose curves of cyst growth and 2D viability for all selected compounds (supplemental figure 4). Thereafter, we made a selection of compounds for which target information was known and that did not lower 2D cell viability below 50% of control. Figure 6A shows images of mIMRFNP-KD 5E4 cysts under control conditions (upper panel) and exposed to test compounds at three concentrations (lower panel). Since these compounds were selected on the condition that 4T1 morphology was not influenced, we provide image data of compound-treated and solvent-treated 4T1 cells in figure 6B. Under solvent conditions, 4T1 cell clumps displayed invasive branching morphology, which was not altered after exposure to VCC03, -18, -23, -55, -73 and -91 at any of the concentrations shown here. VCC55 affected 4T1 morphology at concentrations above 100nM, which was indeed consistent with our phenotypic classification shown in figure 5E. Similarly, VCC73 inhibited cyst growth without affecting 4T1 morphology at 10nM, but affected both 2D cell viability and 4T1 morphology at concentrations ≥100nM.

Discussion and conclusions

To find selective inhibitors of cyst growth and relate compound efficacy to molecular targets, we screened a kinase inhibitor library using a screening platform that uses mIMRFNPKD 5E4 cells as a model of cystogenesis.[28] Cyst growth could be enhanced by exposure of these cells to cAMP-enhancing compounds such as forskolin and prostaglandin E1. In addition, cyst growth could be enhanced by membrane permeable 8-Br-cAMP, indicating that the increase in cyst growth is indeed due to increased levels

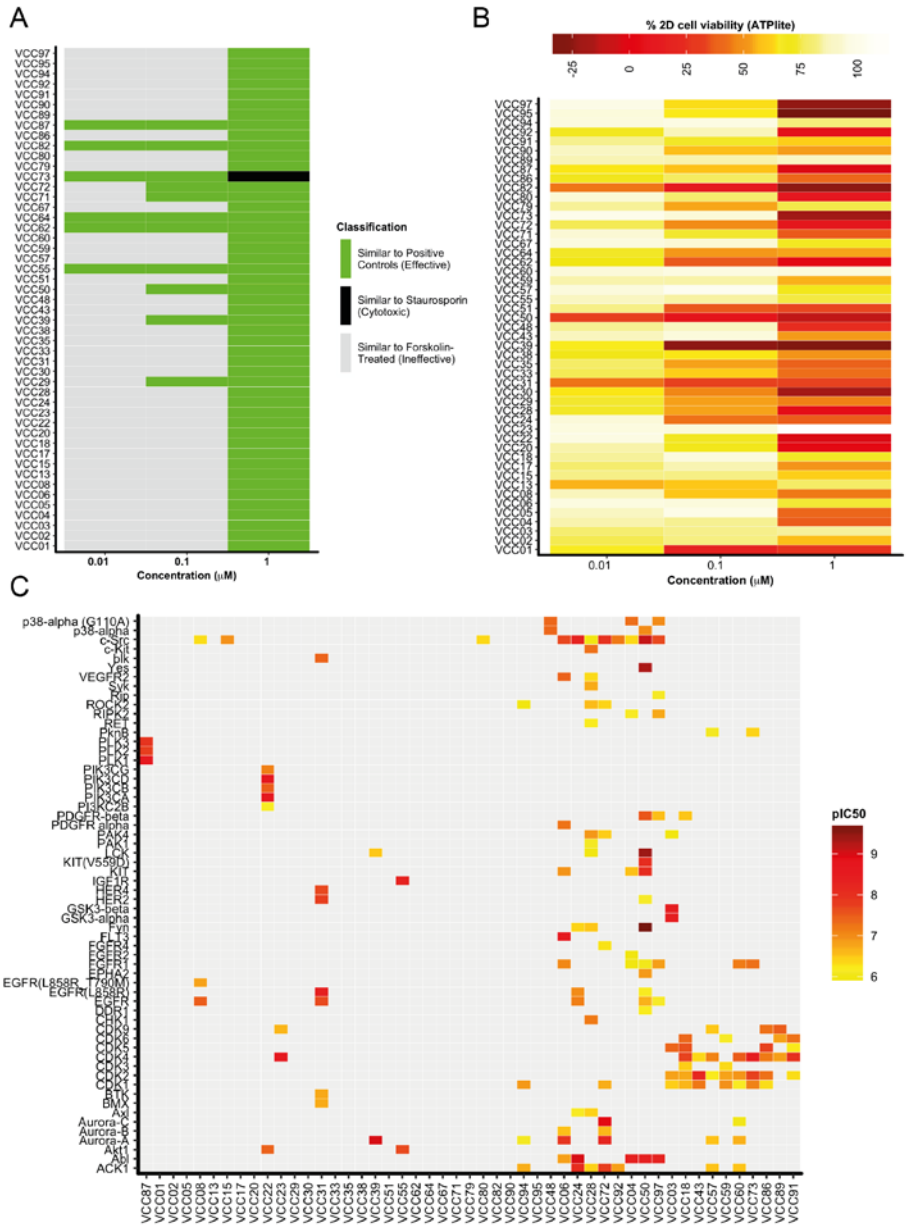

FIGURE 4 Compounds that show low toxicity in 3D cultured mIMRFNPKD 5E4 cells have broad target space. A) Selection of compounds from 3C that do not induce staurosporin-like phenotypic changes. Selection criteria: (i) non-staurosporin-like at any concentration or (ii) if at any concentration staurosporin-like, also effective at two lower concentrations (≥2/3 or replicates for all criteria). **B)** 2D ATPlite on mIMRFNPKD 5E4 represented by yellow to red colour scale. While these compounds do not show toxicity in 3D cysts, they may affect 2D viability. **C)** Target spectrum belonging to

(legend continues on next page)

compounds shown in A. pIC50 shown as colour scale from yellow (µM IC50) to red (≤nM IC50). Unknown target specificity represented by grey background colour. IC50 values >1µM excluded from this list and presented as grey colour.

of intracellular cAMP, in line with previous findings.[46] As expected, inhibitors that disrupted pathways important in PKD, such as mammalian target of rapamycin (mTOR)[34-38] (rapamycin), CDKs[39-41] (roscovitine) and vascular endothelial growth factor receptor (VEGFR)/Raf[43-45] (sorafenib), also inhibited cyst growth in our model, consistent with our previous observations.[28] After assay characterisation, we screened a kinase inhibitor library of 428 compounds to identify cyst growth inhibitors and relate activity to molecular targets. From our screen, we selected 99 cyst growth-inhibiting compounds that were re-screened at three concentrations, confirming the efficacy of 90/99 compounds. The identification of such a large number of effective cyst growth inhibitors was not entirely surprising, since many compounds in the library were either multikinase inhibitors and/or inhibitors of various CDKs at the tested concentrations and had overlapping kinases among their targets.

In order to exclude potentially cytotoxic compounds, we further analysed the phenotypic changes that occurred in mIMRFNPKD 5E4 cysts after compound exposure. Staurosporin is a known inducer of cell death by apoptosis[47] due to its inhibition of multiple kinases,[48] and was therefore included as a positive control for cytotoxicity in our screen, since we reasoned that compounds similar to staurosporin are unlikely to become a drug for PKD. We could therefore classify the phenotypic changes as 'staurosporin-like', 'similar to positive control' or as 'similar to forskolin-treated'. Many compounds classifying as 'staurosporin-like' also lowered cell viability in 2D culture, supporting this toxic classification. Upon prioritisation of compounds that did not induce phenotypic changes associated with staurosporin-like toxicity, we noticed that many of the selected compounds inhibit targets that were previously considered to play a role in cystogenesis. For example, VCC31 inhibited HER2, which was previously implicated in PKD[49] as well as epidermal growth factor receptor (EGFR)[50] at the tested concentrations, and VCC55 inhibited the IGF1R, a target previously identified as potential mediator of cyst growth[51-52] and Akt1. To our surprise, many multikinase inhibitors such as VCC06, -24, -28, -72, or -50 also showed potent efficacy at inhibiting cyst growth, while not causing detectable cytotoxicity in our 3D cyst assay.

Because we used staurosporin as a model compound for cytotoxicity, our phenotypic classification of cytotoxicity is limited to the morphological characteristics we observed of staurosporin-treated cysts. We cannot exclude the possibility that cellular toxicity is exerted through multiple different phenotypic changes, and it is therefore unclear how this classification would perform in the identification of toxic compounds that have a different mechanism of general toxicity compared to staurosporin (e.g. inhibiting survival signalling). This may explain our observation that some compounds impaired viability of 2D-cultured cells, while no toxicity was observed in 3D-cultured

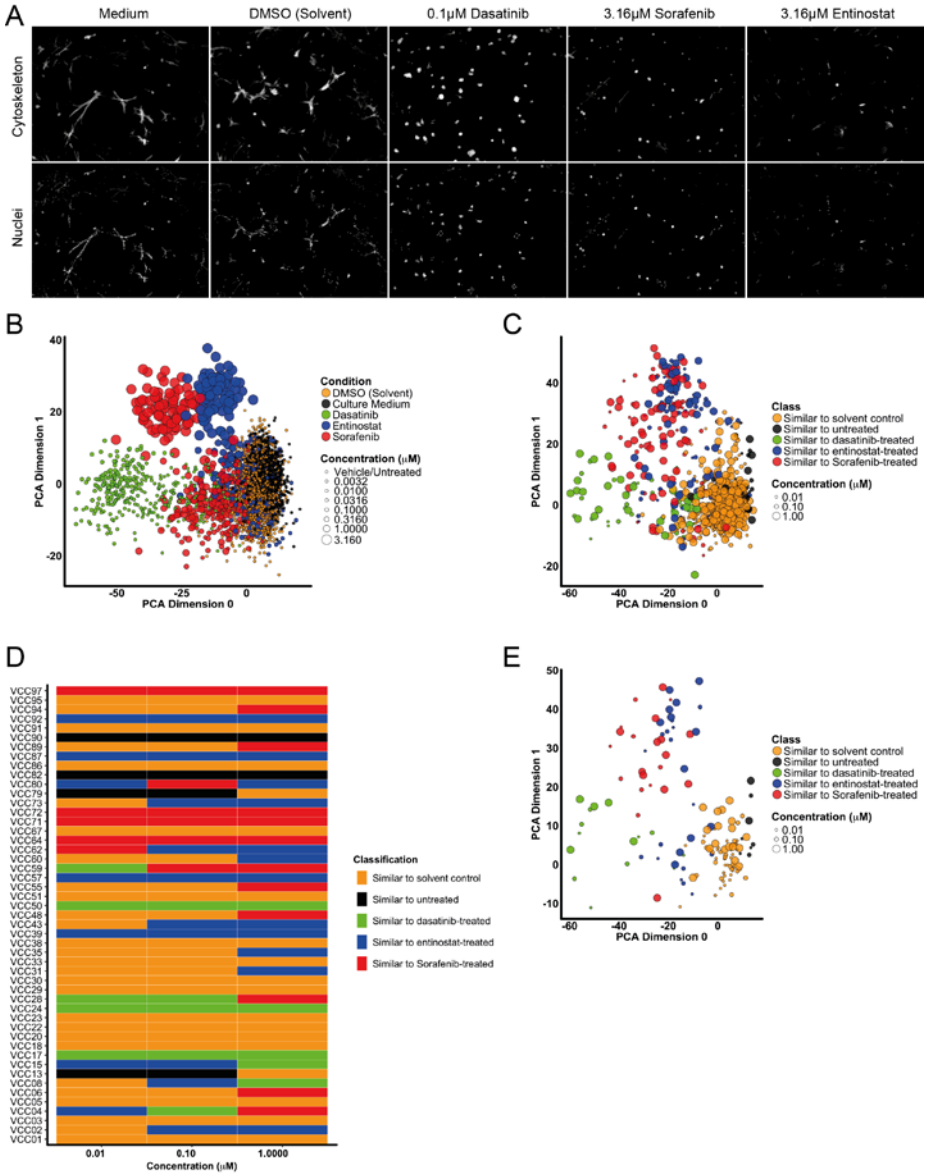

FIGURE 5 Counter screening with 4T1 tumour cells identifies selective inhibitors of cytogenesis. A) Representative images of 4T1 under control conditions obtained with the BD Pathway 855 imager. Contrast and brightness were enhanced for presentation purposes. **B)** Control compounds can be discriminated using PCA analysis. Two principal components (67% of variation) shown for presentation purposes. Circles represent individual wells. **C)** 428 Vichem compounds (at 1µM, 100nM and 10nM) classified using K nearest neighbour classification trained on control compounds using PCA. Two principal components (67% of variation) shown for presentation

(legend continues on next page)

purposes. Circles represent median values of quadruplicate wells. **D)** Heatmap plot with classification of compounds shown in figure 4A. **E)** PCA plot as in figure C, but showing only molecules presented in figure D (molecules that inhibited cyst growth in our PKD assay). Circles represent median of quadruplicate wells and circle size corresponds to concentration.

TABLE 1 Hit compounds inhibiting cystogenesis but not affecting tumour cell invasion: described targets with pIC50>6.0

VCCID	*Target 1 (pIC50)*	*Target 2 (pIC50)*	*Target 3 (pIC50)*	*Target 4 (pIC50)*	*Target 5 (pIC50)*	*Target 6 (pIC50)*	*Target 7 (pIC50)*
VCC01	-	-	-	-	-	-	-
VCC03	GSK3-alpha (8.4)	GSK3-beta (8.4)	CDK5 (7.4)	CDK2 (6.8)	CDK1 (6.44)	PAK4 (6.01)	-
VCC05	-	-	-	-	-	-	-
VCC13	-	-	-	-	-	-	-
VCC18	CDK4 (7.73)	CDK5 (7.59)	CDK6 (7.36)	CDK2 (6.73)	CDK1 (6.63)	PDGFR-beta (6.5)	CDK3 (6.44)
VCC20	-	-	-	-	-	-	-
VCC22	PIK3CA (8.52)	PIK3CD (8.52)	PIK3CB (7.48)	Akt1 (7.44)	PIK3CG (7.12)	PI3KC2B (6.17)	-
VCC23	CDK4 (8.62)	CDK9 (6.63)	-	-	-	-	-
VCC29	-	-	-	-	-	-	-
VCC30	-	-	-	-	-	-	-
VCC33	-	-	-	-	-	-	-
VCC38	-	-	-	-	-	-	-
VCC51	-	-	-	-	-	-	-
VCC55	IGF1R (8.3)	Akt1 (7.66)	-	-	-	-	-
VCC67	-	-	-	-	-	-	-
VCC73	CDK4 (8.4)	CDK2 (7.76)	FGFR1 (7.29)	CDK1 (7.1)	PknB (6.4)	-	-
VCC79	-	-	-	-	-	-	-
VCC82	-	-	-	-	-	-	-
VCC86	CDK5 (7.74)	CDK2 (7.28)	CDK9 (7.28)	CDK4 (7.17)	CDK1 (6.31)	-	-
VCC90	-	-	-	-	-	-	-
VCC91	CDK4 (7.96)	CDK6 (7.26)	CDK2 (6.31)	CDK5 (6.21)	-	-	-
VCC95	-	-	-	-	-	-	-

cysts (e.g. VCC50) – although this could also be explained by the large differences between 3D- and 2D cell cultures.[15, 17] Another limitation associated with the classification of cytotoxicity according to staurosporin-treated cysts, as we performed here, is that we only assessed cytotoxicity on one cell type. Because tissues in the human body are constructed of a tightly regulated functional network of many different cell types and surrounding matrix, it is unclear how our observations relate to the organ toxicity that often causes drug withdrawal. An interesting approach to mapping these phenotypic effects of different toxic chemicals across different cell types, would be to compose a compound library containing compounds with various different mechanisms of cellular toxicity (such as inhibitors of cell cycle progression, inhibitors of survival signalling pathways, DNA-damaging agents or chemicals interfering with energy metabolism). This would enable the classification of the resulting phenotypic changes across multiple cell types (e.g. hepatocytes, cardiomyocytes, endothelial cells, or even co-cultures). Such an effort could potentially alleviate the requirement of performing viability measurements in 2D-cultured cells in parallel. Additionally, mapping the phenotypic alterations that occur from different cytotoxic compounds could contribute to classification of (cytotoxic) compounds in compound libraries other than the screened kinase inhibitor library, and help in the pre-selection of better drugs.

To filter out compounds that may affect other processes than cyst swelling, we therefore performed a counter-screen of the same compound library in a 4T1-cell based tumour invasion assay. This allowed us to prioritise compounds that affected mIMRFNPKD 5E4 cyst growth, but not 4T1 growth and invasion. Importantly, activity of a compound on 4T1 growth and invasion does not necessarily exclude the potential for it to be useful as a treatment against PKD, as cyst growth is also, at least in part, the result of increased proliferation and changes in cell polarity.[53] As a result of this stringent prioritization on 4T1 morphology, we selected 22 compounds that interfered solely with forskolin-induced cyst swelling, but not with 4T1 morphology, although potential false-negatives in our 4T1 counter screen were not taken into consideration. Interestingly, this selection caused exclusion of compounds VCC06, -24, -28, -72 and -50, that were mentioned above as multikinase inhibitors. It is likely that these compounds affected both cystogenesis and 4T1 morphology due to their ability to affect multiple kinases and pathways.

Out of the 22 compounds that were classified as selective cyst growth inhibitors, molecular targets and IC50 values were pre-determined only for 8 compounds (Table 1). An interesting observation is that many of these compounds inhibited various cyclin-depended kinases (CDKs), such as VCC03, -18, -23, -73, -86 and VCC91, which is also corresponds with our previous results.[28] These compounds generally inhibited CDKs involved in transition through the different phases of the cell-division cycle (CDK1, CDK2, CDK4 and CDK6), or in the case of VCC23 and VCC86, also inhibit CDK9, which can phosphorylate RNA polymerase II, thereby modulating transcription.[54] Additionally, inhibitory activity towards CDK5 (VCC03, -18, -86 and -91) may be of particular interest in PKD due to its involvement in regulating ciliary length and cystic

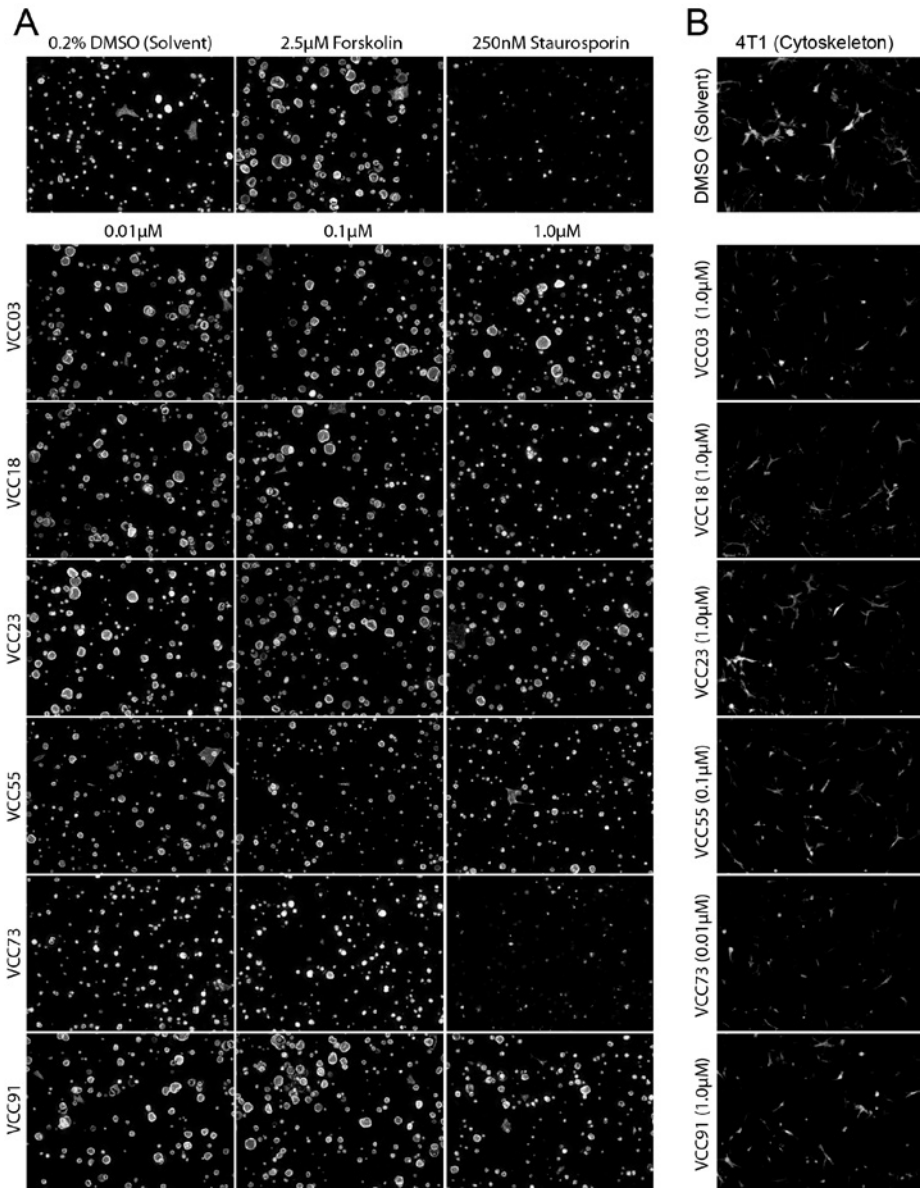

FIGURE 6 Several compounds inhibit cystogenesis without affecting 4T1 phenotype. **A)** Representative images of control conditions (upper panel) and VCC03, VCC18, VCC23, VCC55, VCC73 and VCC91 in three different concentrations (lower panel). Images were taken using an ImageXpress Micro XLS imager. 600x450px cut-out shown of cytoskeleton images. Contrast and brightness are enhanced for presentation purposes. **B)** Representative images of 4T1 phenotype after exposure to compounds from A. Images taken with a BD Pathway 855 imager. Cytoskeleton shown and contrast and brightness increased for presentation purposes.

disease progression.[55] Likewise, CDK inhibitors such as roscovitine and CR8 have been assessed for efficacy in PKD models on several occasions,[40-41] these tests have not culminated in clinical trials due to safety with these anticancer drugs for long-term treatment of PKD.[56-57] It is also important to note that while many CDK inhibitors were found to be active without causing obvious toxicity in this assay, many other CDK inhibitors were excluded on the basis of toxicity and/or effects on 4T1 cells. Because cell proliferation is an important contributor to cyst growth, inhibition of CDKs for the treatment of PKD may be attractive if, for example, renal targeting can be achieved, if the dosage required to prevent cyst swelling is not associated with side effects, or if more selective CDK inhibitors can be used against CDKs directly implicated in the signalling of polycystin proteins or cystic disease (such as CDK2[58] or CDK5[55]). In addition to CDKs, some compounds also targeted fibroblast growth factor receptor 1 (FGFR1, VCC73) or platelet-derived growth factor receptor-beta (PDGFR-beta, VCC18) which are potentially involved in deciliation and could therefore have relevance to cyst formation,[59-60] although it is currently uncertain if these receptors are expressed in mIMRFNPKD 5E4 cells. However, because these two compounds also potently inhibited various CDKs, it is more likely that the observed effects of these compounds were exerted through CDKs, rather than through FGFR1 or PDGFR-beta. Similarly, VCC03, in addition to targeting several CDKs, is also known to inhibit GSK3α/β. GSK3β has been described to be involved in ciliary maintenance,[61] although GSK3-targeted therapy is also likely to affect multiple tissues and may have side effects in different organs.[62]

Interestingly, we found one molecule (VCC55) that inhibited both IGF1R and Akt1. The involvement of IGF1R in cystogenesis was previously reported[63] and is also in line with our previous findings.[32] However, we also observed potent inhibitory activity in the micromolar range of one PI3K/Akt inhibitor, VCC22, which contradicts our previous findings where we screened a panel of PI3K inhibitors and failed to observe a potent effect.[28] Because VCC22 has a high affinity for Akt1 (pIC50 of 7.44), a potential explanation for its efficacy is that the observed effects of this compound are mediated through Akt-mTOR, rather than through PI3K. An additional interesting finding was that many compounds inhibiting targets previously implicated in PKD, such as the vascular endothelial growth factor receptor (VEGFR),[64] EGFR[50] and Aurora A kinase,[65-66] were not selected as selective inhibitors of cyst growth, since these inhibitors often also influenced 4T1 cell morphology or lacked efficacy altogether. While currently the compounds that were identified as selective cyst growth inhibitors in our assays do not reveal new targets to modulate cyst growth, full characterisation of the compounds with undescribed target specificity could elucidate the mechanistic effects that reduced cyst growth.

Because the 22 compounds we described were identified using a PKD assay that uses a murine cell line (mIMRFNPKD 5E4), it is necessary to validate the efficacy of these molecules in a human PKD model. A possibility for this validation is to use a human kidney cell line, although ideally this should be performed using primary human cystic tissue. Such an effort could be used to exclude the possibility that the identified molecules show preferential inhibition in murine cell lines and account for differences

in receptor specificity between murine and human cells.

In conclusion, by testing a kinase inhibitor library using phenotypic screening on 3D-cultured cysts we identified inhibitors of cyst growth, that could be classified according to their predicted toxic effects. Upon counter-selection in a second 3D cell culture model using 4T1 tumour cells, selective inhibitors of cyst growth could be identified based on lack of activity towards 4T1 cells. These compounds are known to target CDKs, IGF1R and others, and future research should focus on the elucidation of the mechanism of action of those compounds where target specificity is currently unknown, in order to potentially identify new modulators of cystogenesis.

Acknowledgments

The authors would like to thank our collaborators at Vichem Chemie Research Ltd, Hungary for providing a small-molecule compound library and target selectivity profiles.

Funding statement

T.H. Booij was supported by the Dutch Technology Foundation STW, project 11823. STW is part of NWO (Netherlands Organization for Scientific Research). The other authors received no financial support for the research or authorship.

Statement of conflicting interests

Leo S. Price is founder and major shareholder of OcellO B.V., a company that provides 3D tissue culture-based screening services. Kuan Yan and Hester Bange are employees of OcellO B.V. The other authors declared no potential conflicts of interest with respect to research or authorship.

References

1. Willey CJ, Blais JD, Hall AK, Krasa HB, Makin AJ, Czerwiec FS: Prevalence of autosomal dominant polycystic kidney disease in the European Union. *Nephrology, dialysis, transplantation : official publication of the European Dialysis and Transplant Association - European Renal Association*, 2016
2. Sommerer C, Zeier M: Clinical Manifestation and Management of ADPKD in Western Countries. *Kidney diseases (Basel, Switzerland)* 2(3): 120-127, 2016
3. Ong AC, Harris PC: A polycystin-centric view of cyst formation and disease: the polycystins revisited. *Kidney international* 88(4): 699-710, 2015
4. Seeger-Nukpezah T, Geynisman DM, Nikonova AS, Benzing T, Golemis EA: The hallmarks of cancer: relevance to the pathogenesis of polycystic kidney disease. *Nature reviews Nephrology* 11(9): 515-534, 2015
5. Saigusa T, Bell PD: Molecular pathways and therapies in autosomal-dominant polycystic kidney disease. *Physiology (Bethesda, Md)* 30(3): 195-207, 2015
6. Baur BP, Meaney CJ: Review of tolvaptan for autosomal dominant polycystic kidney disease. *Pharmacotherapy* 34(6): 605-616, 2014

7. Higashihara E, Torres VE, Chapman AB, Grantham JJ, Bae K, Watnick TJ, Horie S, Nutahara K, Ouyang J, Krasa HB, Czerwiec FS: Tolvaptan in autosomal dominant polycystic kidney disease: three years' experience. *Clinical journal of the American Society of Nephrology : CJASN* 6(10): 2499-2507, 2011
8. Torres VE, Chapman AB, Devuyst O, Gansevoort RT, Grantham JJ, Higashihara E, Perrone RD, Krasa HB, Ouyang J, Czerwiec FS: Tolvaptan in patients with autosomal dominant polycystic kidney disease. *The New England journal of medicine* 367(25): 2407-2418, 2012
9. Woodhead JL, Brock WJ, Roth SE, Shoaf SE, Brouwer KL, Church R, Grammatopoulos TN, Stiles L, Siler SQ, Howell BA, Mosedale M, Watkins PB, Shoda LK: Application of a Mechanistic Model to Evaluate Putative Mechanisms of Tolvaptan Drug-Induced Liver Injury and Identify Patient Susceptibility Factors. *Toxicological sciences : an official journal of the Society of Toxicology* 155(1): 61-74, 2017
10. Watkins PB, Lewis JH, Kaplowitz N, Alpers DH, Blais JD, Smotzer DM, Krasa H, Ouyang J, Torres VE, Czerwiec FS, Zimmer CA: Clinical Pattern of Tolvaptan-Associated Liver Injury in Subjects with Autosomal Dominant Polycystic Kidney Disease: Analysis of Clinical Trials Database. *Drug safety* 38(11): 1103-1113, 2015
11. Fang JL, Wu Y, Gamboa da Costa G, Chen S, Chitranshi P, Beland FA: Human Sulfotransferases Enhance the Cytotoxicity of Tolvaptan. *Toxicological sciences : an official journal of the Society of Toxicology* 150(1): 27-39, 2016
12. Nagao S, Kugita M, Yoshihara D, Yamaguchi T: Animal models for human polycystic kidney disease. *Experimental animals* 61(5): 477-488, 2012
13. Torres VE, Harris PC: Polycystic kidney disease: genes, proteins, animal models, disease mechanisms and therapeutic opportunities. *Journal of internal medicine* 261(1): 17-31, 2007
14. Wilson PD: Mouse models of polycystic kidney disease. *Current topics in developmental biology* 84 311-350, 2008
15. Debnath J, Brugge JS: Modelling glandular epithelial cancers in three-dimensional cultures. *Nature reviews Cancer* 5(9): 675-688, 2005
16. Fischbach C, Chen R, Matsumoto T, Schmelzle T, Brugge JS, Polverini PJ, Mooney DJ: Engineering tumors with 3D scaffolds. *Nature methods* 4(10): 855-860, 2007
17. Birgersdotter A, Sandberg R, Ernberg I: Gene expression perturbation in vitro--a growing case for three-dimensional (3D) culture systems. *Seminars in cancer biology* 15(5): 405-412, 2005
18. Benam KH, Dauth S, Hassell B, Herland A, Jain A, Jang KJ, Karalis K, Kim HJ, MacQueen L, Mahmoodian R, Musah S, Torisawa YS, van der Meer AD, Villenave R, Yadid M, Parker KK, Ingber DE: Engineered in vitro disease models. *Annual review of pathology* 10 195-262, 2015
19. Desrochers TM, Palma E, Kaplan DL: Tissue-engineered kidney disease models. *Advanced drug delivery reviews* 69-70 67-80, 2014
20. Santo VE, Rebelo SP, Estrada MF, Alves PM, Boghaert E, Brito C: Drug screening in 3D in vitro tumor models: overcoming current pitfalls of efficacy read-outs. *Biotechnology journal* 12(1), 2017

21. Kimlin L, Kassis J, Virador V: 3D in vitro tissue models and their potential for drug screening. *Expert opinion on drug discovery* 8(12): 1455-1466, 2013
22. DesRochers TM, Suter L, Roth A, Kaplan DL: Bioengineered 3D human kidney tissue, a platform for the determination of nephrotoxicity. *PloS one* 8(3): e59219, 2013
23. Fuchs TC, Hewitt P: Biomarkers for drug-induced renal damage and nephrotoxicity- an overview for applied toxicology. *The AAPS journal* 13(4): 615-631, 2011
24. Lazarou J, Pomeranz BH, Corey PN: Incidence of adverse drug reactions in hospitalized patients: a meta-analysis of prospective studies. *Jama* 279(15): 1200-1205, 1998
25. Uetrecht J, Naisbitt DJ: Idiosyncratic adverse drug reactions: current concepts. *Pharmacological reviews* 65(2): 779-808, 2013
26. Horvath P, Aulner N, Bickle M, Davies AM, Nery ED, Ebner D, Montoya MC, Ostling P, Pietiainen V, Price LS, Shorte SL, Turcatti G, von Schantz C, Carragher NO: Screening out irrelevant cell-based models of disease. *Nature reviews Drug discovery* 15(11): 751-769, 2016
27. Tsai SQ, Wyvekens N, Khayter C, Foden JA, Thapar V, Reyon D, Goodwin MJ, Aryee MJ, Joung JK: Dimeric CRISPR RNA-guided FokI nucleases for highly specific genome editing. *Nature biotechnology* 32(6): 569-576, 2014
28. Booij TH, Bange H, Leonhard WN, Yan K, Fokkelman M, Kunnen SJ, Dauwerse JG, Qin Y, van de Water B, van Westen GJP, Peters DJM, Price LS: High-Throughput Phenotypic Screening of Kinase Inhibitors to Identify Drug Targets for Polycystic Kidney Disease. *SLAS Discov* 2472555217716056, 2017
29. Di Z, Klop MJ, Rogkoti VM, Le Devedec SE, van de Water B, Verbeek FJ, Price LS, Meerman JH: Ultra high content image analysis and phenotype profiling of 3D cultured micro-tissues. *PloS one* 9(10): e109688, 2014
30. Gyorgy K, Laszlo O, Daniel E, Balint H-B, Csaba S-K, Zoltan H, Frigyes W, Jeno M, Istvan S, Janos P, Zoltan G, Doris H, Henrik D, Gerhard M, Bert K, Axel U: Signal Transduction Therapy with Rationally Designed Kinase Inhibitors. *Current Signal Transduction Therapy* 1(1): 67-95, 2006
31. Keri G, Szekelyhidi Z, Banhegyi P, Varga Z, Hegymegi-Barakonyi B, Szantai-Kis C, Hafenbradl D, Klebl B, Muller G, Ullrich A, Eros D, Horvath Z, Greff Z, Marosfalvi J, Pato J, Szabadkai I, Szilagyi I, Szegedi Z, Varga I, Waczek F, Orfi L: Drug discovery in the kinase inhibitory field using the Nested Chemical Library technology. *Assay Drug Dev Technol* 3(5): 543-551, 2005
32. Booij TH, Klop MJ, Yan K, Szantai-Kis C, Szokol B, Orfi L, van de Water B, Keri G, Price LS: Development of a 3D Tissue Culture-Based High-Content Screening Platform That Uses Phenotypic Profiling to Discriminate Selective Inhibitors of Receptor Tyrosine Kinases. *Journal of biomolecular screening* 21(9): 912-922, 2016
33. Edwards SR, Wandless TJ: The rapamycin-binding domain of the protein kinase mammalian target of rapamycin is a destabilizing domain. *J Biol Chem* 282(18): 13395-13401, 2007

34. Shillingford JM, Murcia NS, Larson CH, Low SH, Hedgepeth R, Brown N, Flask CA, Novick AC, Goldfarb DA, Kramer-Zucker A, Walz G, Piontek KB, Germino GG, Weimbs T: The mTOR pathway is regulated by polycystin-1, and its inhibition reverses renal cystogenesis in polycystic kidney disease. *Proc Natl Acad Sci U S A* 103(14): 5466-5471, 2006
35. Novalic Z, van der Wal AM, Leonhard WN, Koehl G, Breuning MH, Geissler EK, de Heer E, Peters DJ: Dose-dependent effects of sirolimus on mTOR signaling and polycystic kidney disease. *Journal of the American Society of Nephrology : JASN* 23(5): 842-853, 2012
36. Kim HJ, Edelstein CL: Mammalian target of rapamycin inhibition in polycystic kidney disease: From bench to bedside. *Kidney research and clinical practice* 31(3): 132-138, 2012
37. Lieberthal W, Levine JS: Mammalian target of rapamycin and the kidney. I. The signaling pathway. *American journal of physiology Renal physiology* 303(1): F1-10, 2012
38. Ren XS, Sato Y, Harada K, Sasaki M, Furubo S, Song JY, Nakanuma Y: Activation of the PI3K/mTOR pathway is involved in cystic proliferation of cholangiocytes of the PCK rat. *PloS one* 9(1): e87660, 2014
39. Meijer L, Borgne A, Mulner O, Chong JP, Blow JJ, Inagaki N, Inagaki M, Delcros JG, Moulinoux JP: Biochemical and cellular effects of roscovitine, a potent and selective inhibitor of the cyclin-dependent kinases cdc2, cdk2 and cdk5. *Eur J Biochem* 243(1-2): 527-536, 1997
40. Bukanov NO, Smith LA, Klinger KW, Ledbetter SR, Ibraghimov-Beskrovnaya O: Long-lasting arrest of murine polycystic kidney disease with CDK inhibitor roscovitine. *Nature* 444(7121): 949-952, 2006
41. Bukanov NO, Moreno SE, Natoli TA, Rogers KA, Smith LA, Ledbetter SR, Oumata N, Galons H, Meijer L, Ibraghimov-Beskrovnaya O: CDK inhibitors R-roscovitine and S-CR8 effectively block renal and hepatic cystogenesis in an orthologous model of ADPKD. *Cell cycle (Georgetown, Tex)* 11(21): 4040-4046, 2012
42. Bach S, Knockaert M, Reinhardt J, Lozach O, Schmitt S, Baratte B, Koken M, Coburn SP, Tang L, Jiang T, Liang DC, Galons H, Dierick JF, Pinna LA, Meggio F, Totzke F, Schachtele C, Lerman AS, Carnero A, Wan Y, Gray N, Meijer L: Roscovitine targets, protein kinases and pyridoxal kinase. *J Biol Chem* 280(35): 31208-31219, 2005
43. Wilhelm SM, Carter C, Tang L, Wilkie D, McNabola A, Rong H, Chen C, Zhang X, Vincent P, McHugh M, Cao Y, Shujath J, Gawlak S, Eveleigh D, Rowley B, Liu L, Adnane L, Lynch M, Auclair D, Taylor I, Gedrich R, Voznesensky A, Riedl B, Post LE, Bollag G, Trail PA: BAY 43-9006 exhibits broad spectrum oral antitumor activity and targets the RAF/MEK/ERK pathway and receptor tyrosine kinases involved in tumor progression and angiogenesis. *Cancer Res* 64(19): 7099-7109, 2004
44. Yamaguchi T, Reif GA, Calvet JP, Wallace DP: Sorafenib inhibits cAMP-dependent ERK activation, cell proliferation, and in vitro cyst growth of human ADPKD cyst epithelial cells. *American journal of physiology Renal physiology* 299(5): F944-951, 2010

45. Sas KM: Targeting B-Raf as a treatment strategy for polycystic kidney disease. *American journal of physiology Renal physiology* 299(5): F942-943, 2010
46. Neufeld TK, Douglass D, Grant M, Ye M, Silva F, Nadasdy T, Grantham JJ: In vitro formation and expansion of cysts derived from human renal cortex epithelial cells. *Kidney international* 41(5): 1222-1236, 1992
47. Belmokhtar CA, Hillion J, Segal-Bendirdjian E: Staurosporine induces apoptosis through both caspase-dependent and caspase-independent mechanisms. *Oncogene* 20(26): 3354-3362, 2001
48. Karaman MW, Herrgard S, Treiber DK, Gallant P, Atteridge CE, Campbell BT, Chan KW, Ciceri P, Davis MI, Edeen PT, Faraoni R, Floyd M, Hunt JP, Lockhart DJ, Milanov ZV, Morrison MJ, Pallares G, Patel HK, Pritchard S, Wodicka LM, Zarrinkar PP: A quantitative analysis of kinase inhibitor selectivity. *Nature biotechnology* 26(1): 127-132, 2008
49. Wilson SJ, Amsler K, Hyink DP, Li X, Lu W, Zhou J, Burrow CR, Wilson PD: Inhibition of HER-2(neu/ErbB2) restores normal function and structure to polycystic kidney disease (PKD) epithelia. *Biochimica et biophysica acta* 1762(7): 647-655, 2006
50. Torres VE, Sweeney WE, Jr., Wang X, Qian Q, Harris PC, Frost P, Avner ED: EGF receptor tyrosine kinase inhibition attenuates the development of PKD in Han:SPRD rats. *Kidney international* 64(5): 1573-1579, 2003
51. Liu C, Zhang Y, Yuan L, Fu L, Mei C: Rosiglitazone inhibits insulin-like growth factor1-induced polycystic kidney disease cell growth and p70S6 kinase activation. *Molecular medicine reports* 8(3): 861-864, 2013
52. Bach LA, Hale LJ: Insulin-like growth factors and kidney disease. *American journal of kidney diseases : the official journal of the National Kidney Foundation* 65(2): 327-336, 2015
53. Happe H, de Heer E, Peters DJ: Polycystic kidney disease: the complexity of planar cell polarity and signaling during tissue regeneration and cyst formation. *Biochimica et biophysica acta* 1812(10): 1249-1255, 2011
54. Malumbres M: Cyclin-dependent kinases. *Genome Biol* 15(6): 122, 2014
55. Husson H, Moreno S, Smith LA, Smith MM, Russo RJ, Pitstick R, Sergeev M, Ledbetter SR, Bukanov NO, Lane M, Zhang K, Billot K, Carlson G, Shah J, Meijer L, Beier DR, Ibraghimov-Beskrovnaya O: Reduction of ciliary length through pharmacologic or genetic inhibition of CDK5 attenuates polycystic kidney disease in a model of nephronophthisis. *Hum Mol Genet* 25(11): 2245-2255, 2016
56. Cicenas J, Kalyan K, Sorokinas A, Stankunas E, Levy J, Meskinyte I, Stankevicius V, Kaupinis A, Valius M: Roscovitine in cancer and other diseases. *Annals of Translational Medicine* 3(10), 2015
57. Song H, Vita M, Sallam H, Tehranchi R, Nilsson C, Siden A, Hassan Z: Effect of the Cdk-inhibitor roscovitine on mouse hematopoietic progenitors in vivo and in vitro. *Cancer chemotherapy and pharmacology* 60(6): 841-849, 2007
58. Bhunia AK, Piontek K, Boletta A, Liu L, Qian F, Xu PN, Germino FJ, Germino GG: PKD1 induces p21(waf1) and regulation of the cell cycle via direct activation of the JAK-STAT signaling pathway in a process requiring PKD2. *Cell* 109(2): 157-168, 2002

59. Pan J, Seeger-Nukpezah T, Golemis EA: The role of the cilium in normal and abnormal cell cycles: emphasis on renal cystic pathologies. *Cellular and molecular life sciences : CMLS* 70(11): 1849-1874, 2013
60. Tucker RW, Scher CD, Stiles CD: Centriole deciliation associated with the early response of 3T3 cells to growth factors but not to SV40. *Cell* 18(4): 1065-1072, 1979
61. Thoma CR, Frew IJ, Hoerner CR, Montani M, Moch H, Krek W: pVHL and GSK3beta are components of a primary cilium-maintenance signalling network. *Nat Cell Biol* 9(5): 588-595, 2007
62. Gray JE, Infante JR, Brail LH, Simon GR, Cooksey JF, Jones SF, Farrington DL, Yeo A, Jackson KA, Chow KH, Zamek-Gliszczynski MJ, Burris HA, 3rd: A first-in-human phase I dose-escalation, pharmacokinetic, and pharmacodynamic evaluation of intravenous LY2090314, a glycogen synthase kinase 3 inhibitor, administered in combination with pemetrexed and carboplatin. *Invest New Drugs* 33(6): 1187-1196, 2015
63. Parker E, Newby LJ, Sharpe CC, Rossetti S, Streets AJ, Harris PC, O'Hare MJ, Ong AC: Hyperproliferation of PKD1 cystic cells is induced by insulin-like growth factor-1 activation of the Ras/Raf signalling system. *Kidney international* 72(2): 157-165, 2007
64. Tao Y, Kim J, Yin Y, Zafar I, Falk S, He Z, Faubel S, Schrier RW, Edelstein CL: VEGF receptor inhibition slows the progression of polycystic kidney disease. *Kidney international* 72(11): 1358-1366, 2007
65. Plotnikova OV, Pugacheva EN, Golemis EA: Aurora A kinase activity influences calcium signaling in kidney cells. *The Journal of cell biology* 193(6): 1021-1032, 2011
66. Nikonova AS, Deneka AY, Eckman L, Kopp MC, Hensley HH, Egleston BL, Golemis EA: Opposing Effects of Inhibitors of Aurora-A and EGFR in Autosomal-Dominant Polycystic Kidney Disease. *Frontiers in oncology* 5 228, 2015

SUPPLEMENTAL MATERIALS

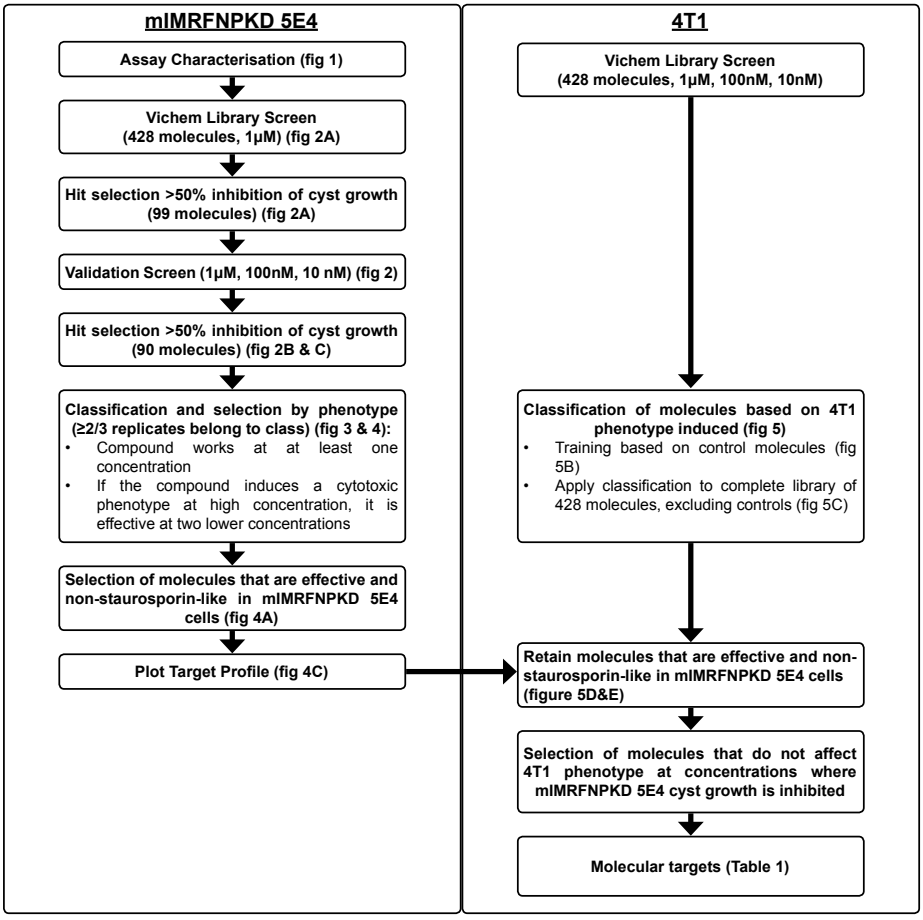

SUPPLEMENTAL FIGURE 1 Data analysis workflow with references to main figures.

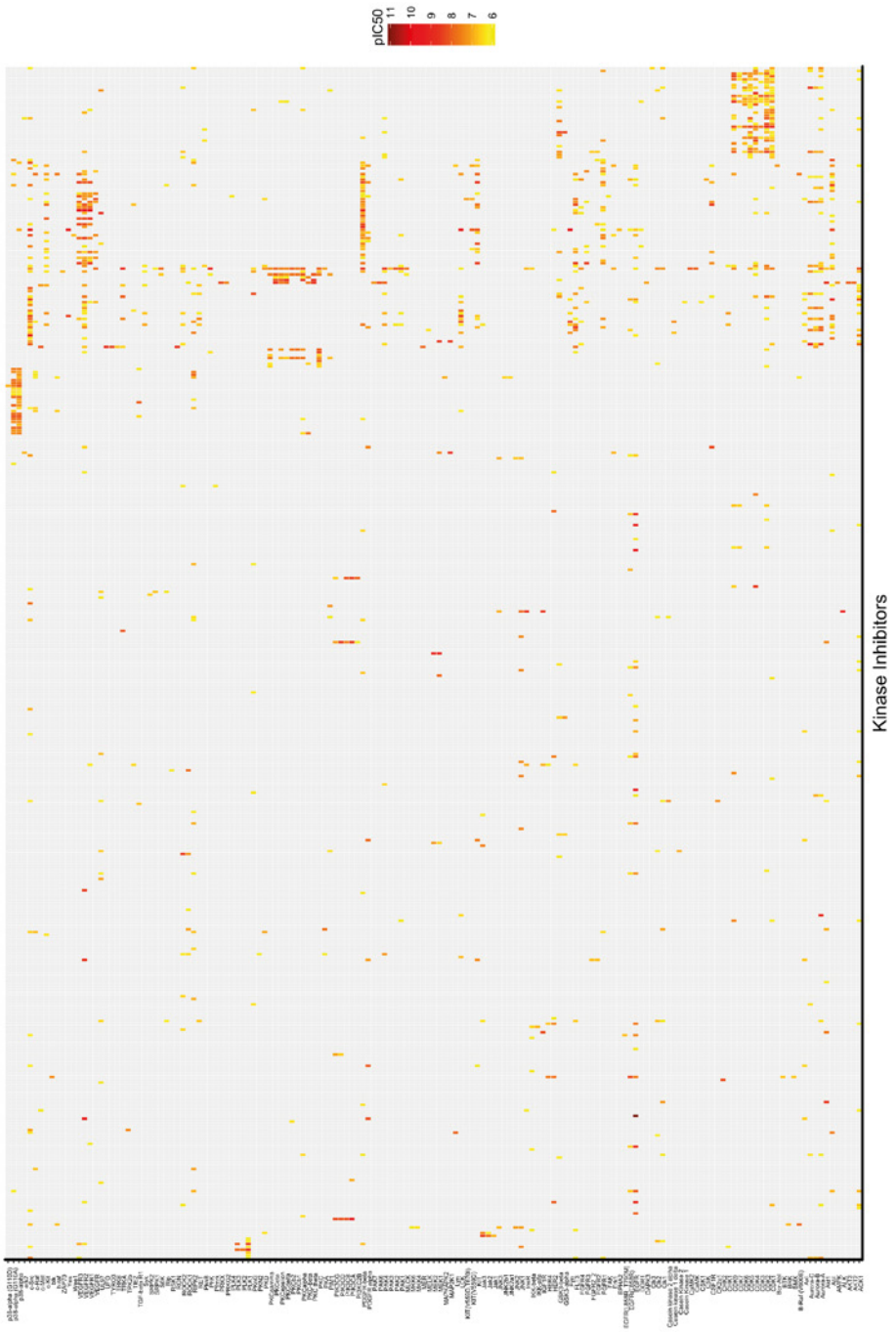

SUPPLEMENTAL FIGURE 2 Target spectrum of all screened compounds with IC50 ≤1uM represented by a yellow to red colour scale.

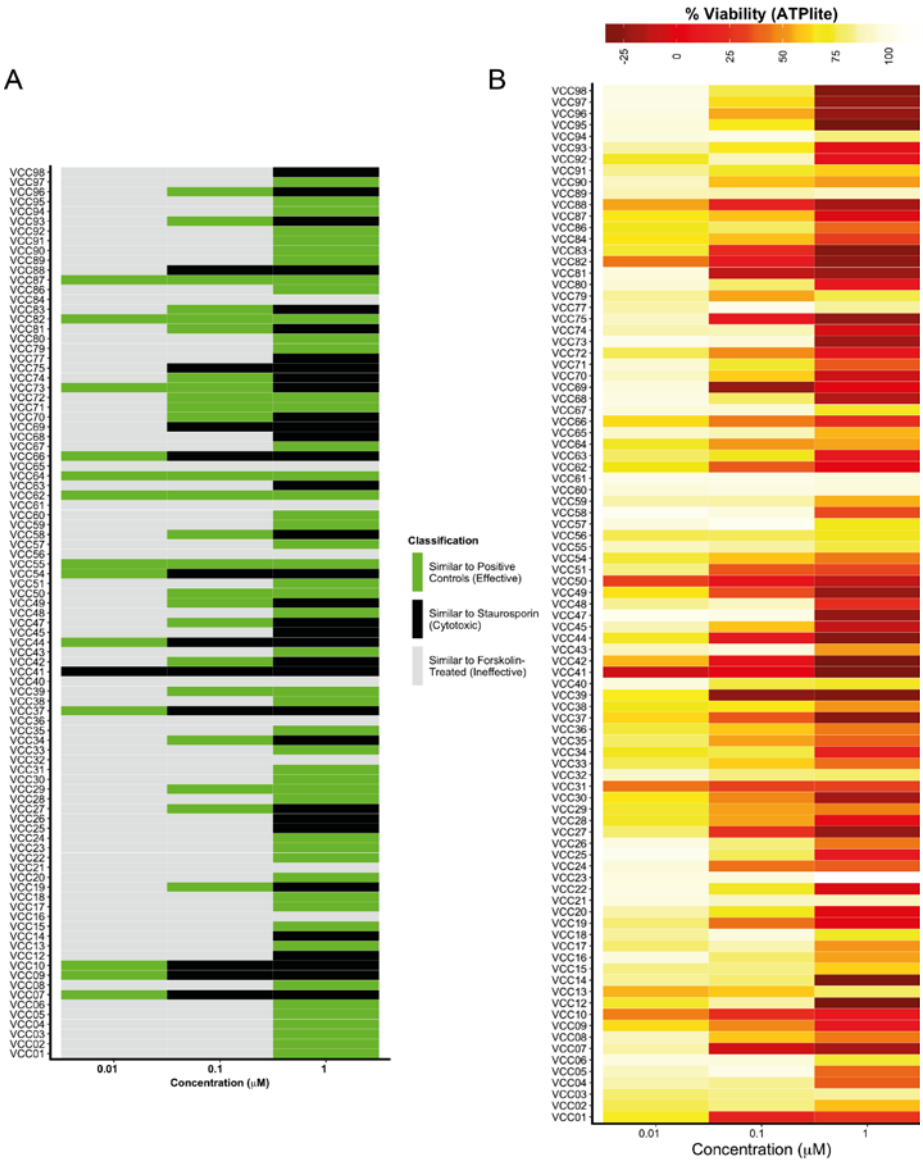

SUPPLEMENTAL FIGURE 3 Correlation of 3D classification using K nearest neighbour classification and 2D cell viability measured by ATPlite. **A)** Heat map showing classification of compounds when ≥2/3 replicates belong to that class. Black colour represents cytotoxic compounds, green represents efficacy and light grey colour represents inactive. **B)** 2D ATPlite on mIMRFNPKD 5E4 represented by yellow to red colour scale. While these compounds do not show toxicity in 3D cysts, they may affect 2D viability.

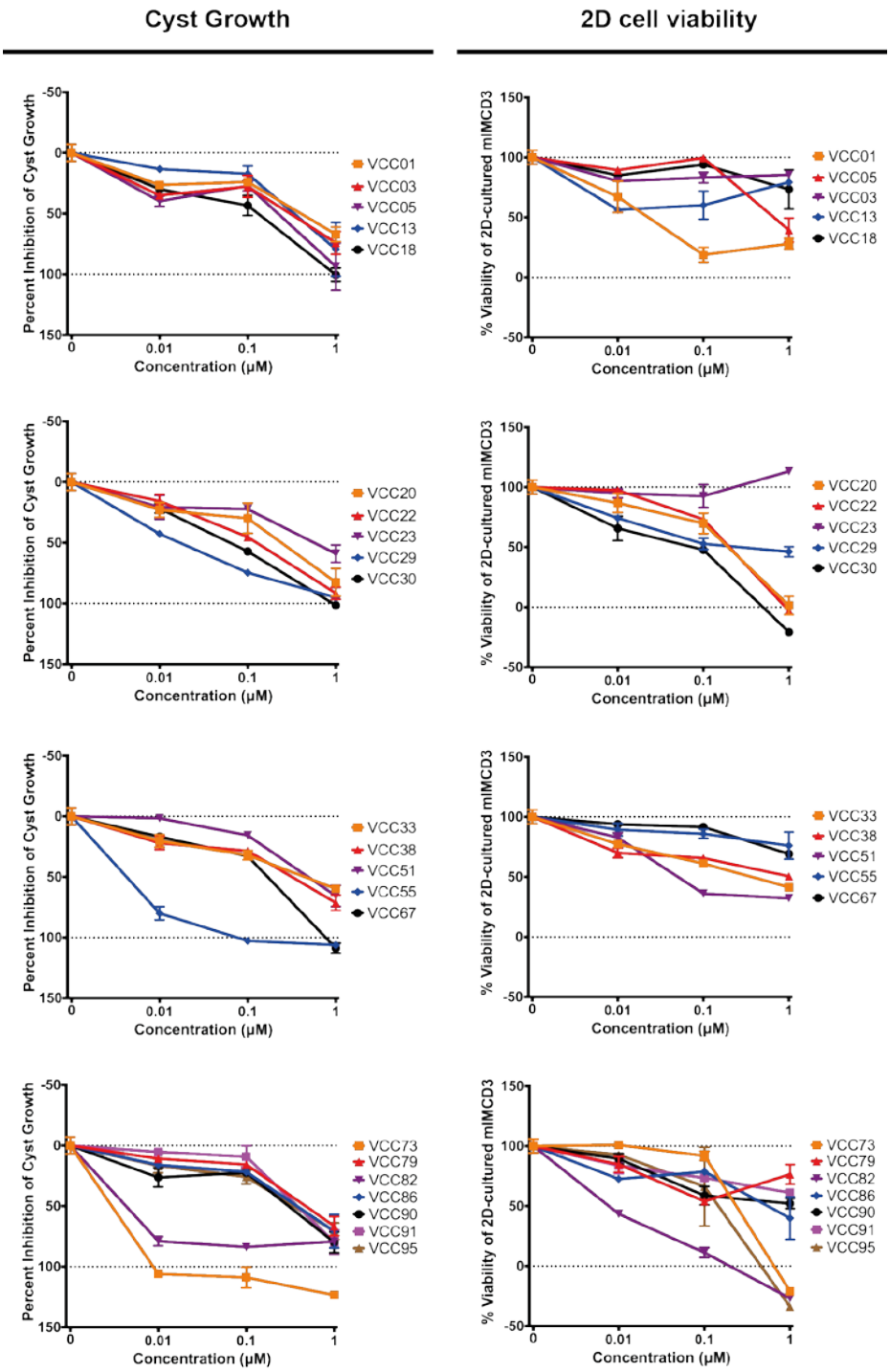
Cyst Growth
2D cell viability
Percent Inhibition of Cyst Growth
% Viability of 2D-cultured mIMCD3
Concentration (μM)
VCC01
VCC03
VCC05
VCC13
VCC18
VCC20
VCC22
VCC23
VCC29
VCC30
VCC33
VCC38
VCC51
VCC55
VCC67
VCC73
VCC79
VCC82
VCC86
VCC90
VCC91
VCC95

‹ SUPPLEMENTAL FIGURE 4 Dose curves for inhibition of cyst growth and 2D cell viability for all compounds presented in figure 5G. Data points represent median ± MAD of triplicate wells. In case error bars are not visible, the MAD is smaller than the point size.